

Supporting Information

Design hierarchical mesoporous/macroporous silicon-based composite anode material for low-cost high-performance lithium-ion batteries

Min Cui[‡], Lin Wang[‡], Xianwei Guo, Errui Wang, Yubo Yang, Tianhao Wu, Di He,

*Shiqi Liu, Haijun Yu**

College of Materials Science and Engineering, Key Laboratory of Advanced Functional Materials, Education Ministry of China, Beijing University of Technology, Beijing 100124, P.R. China

*E-mail: hj-yu@bjut.edu.cn

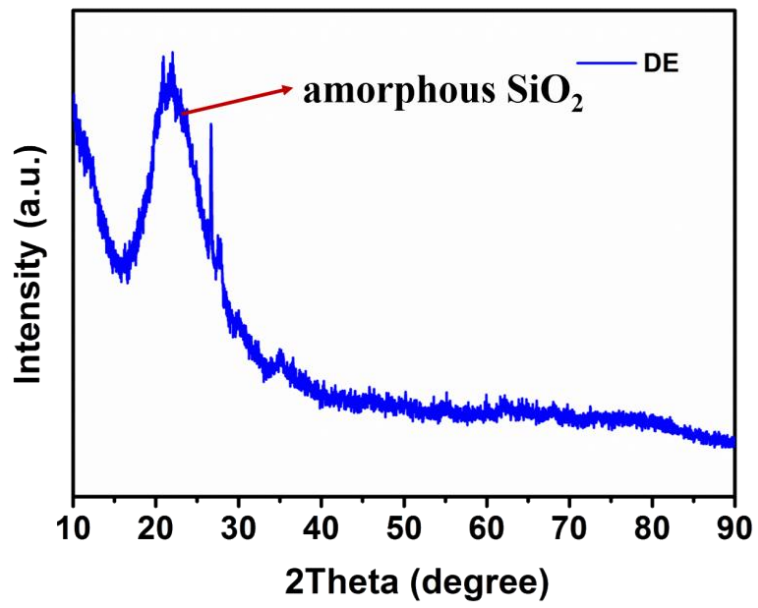


Fig.S1 XRD pattern of the DE. Vertical bars indicate peak position and intensity of SiO₂.

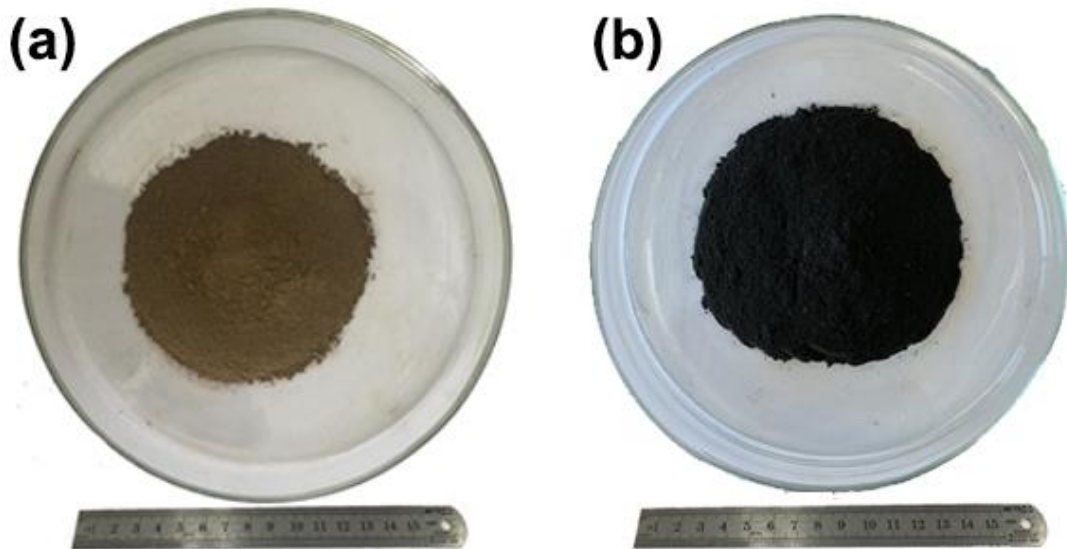


Fig.S2 The photograph of the mass-produced materials (a) hierarchical porous Si/SiO₂; (b) hierarchical porous Si/SiO₂@C composite materials.

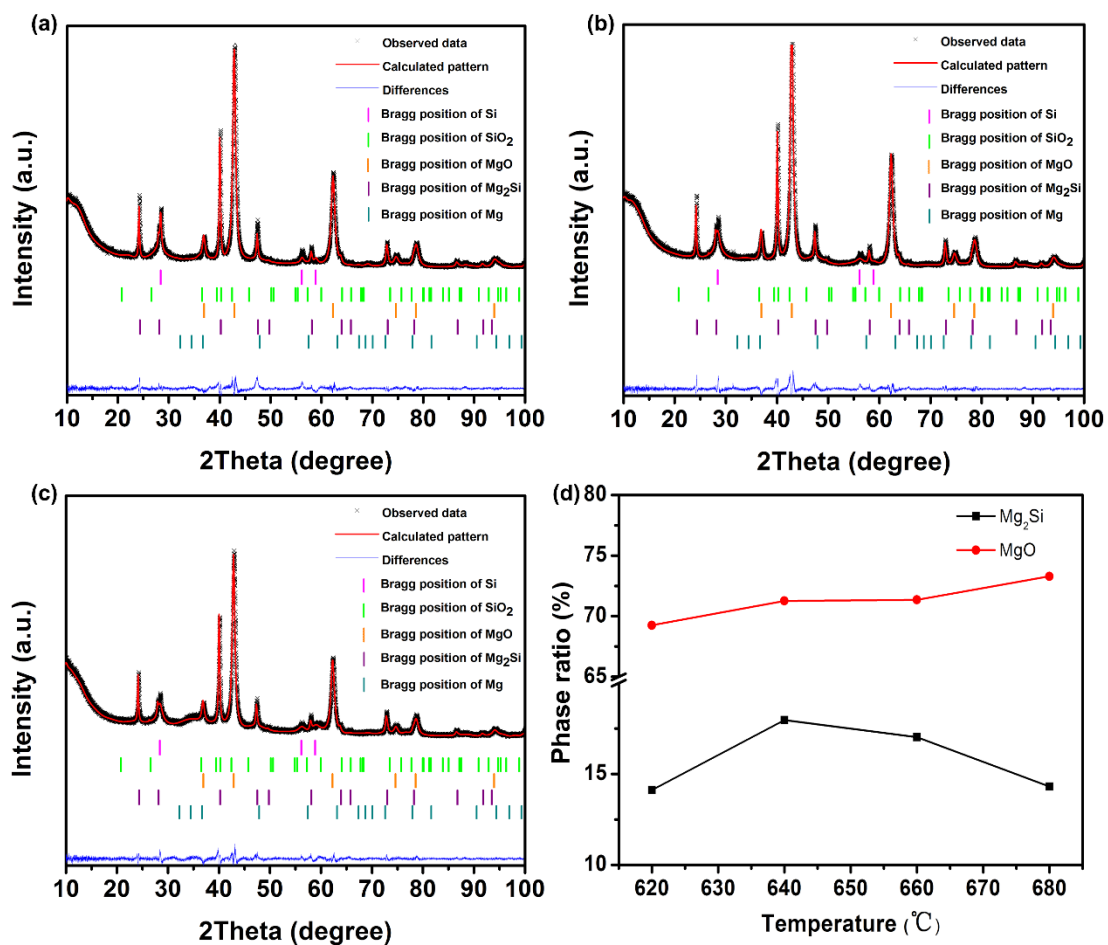


Fig.S3 XRD pattern of the samples and Rietveld refinement results after magnesiothermic reduction under different temperature for 1 h after washing in water, (a) 620°C; (b) 660°C; (c) 680°C. (d) The phase ratio of the Mg₂Si and MgO after magnesiothermic reduction under the temperature of 620°C, 640°C, 660°C and 680°C, respectively.

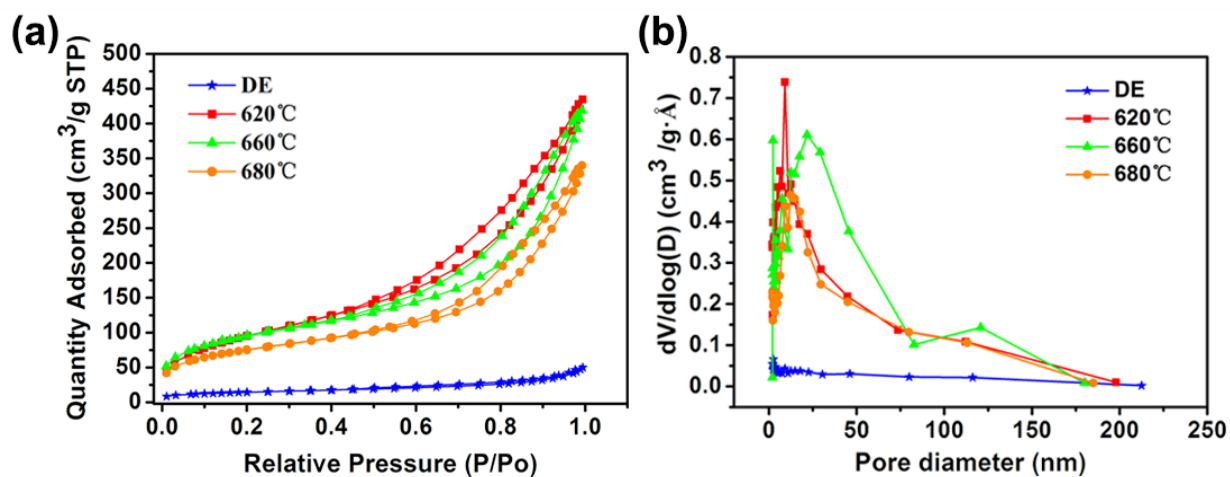


Fig.S4 (a) N_2 adsorption/desorption isotherm curves of the DE and hierarchical mesoporous/macroporous structure Si/SiO₂ samples after magnesiothermic reduction under different temperature. (b) The Barrett-Joyner-Halenda (BJH) pore size distributions from adsorption branches of the isotherm.

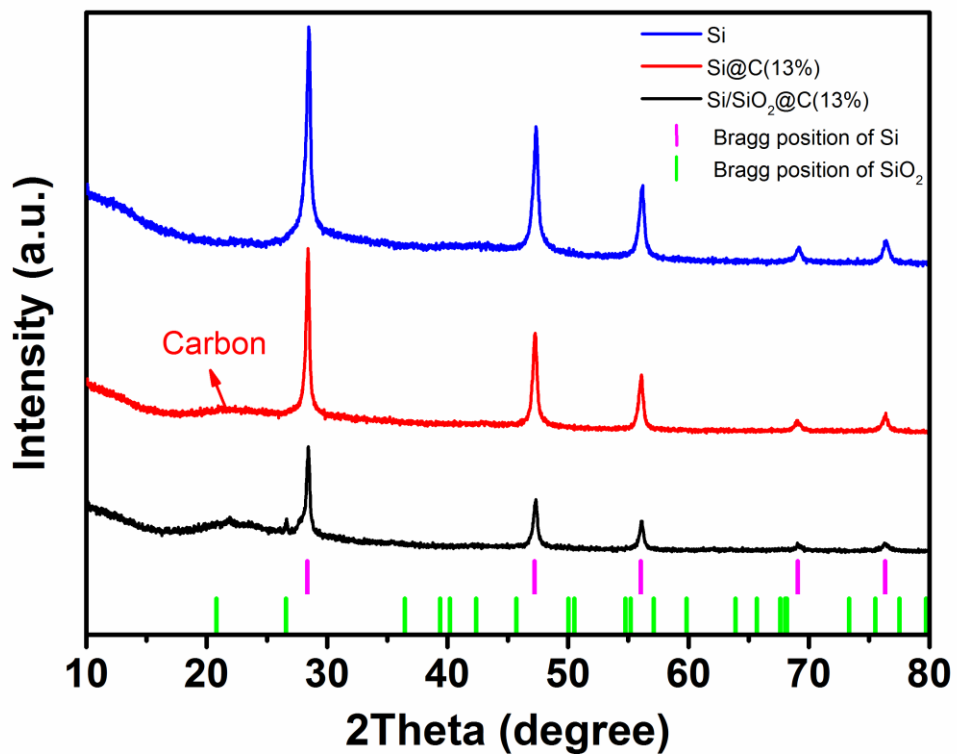


Fig.S5 XRD patterns of the Si after magnesiothermic reduction under 750°C for 5 h, Si@C (13%) composite material and Si/SiO₂@C (13%) composite material. Vertical bars indicate peak position and intensity of Si and SiO₂.

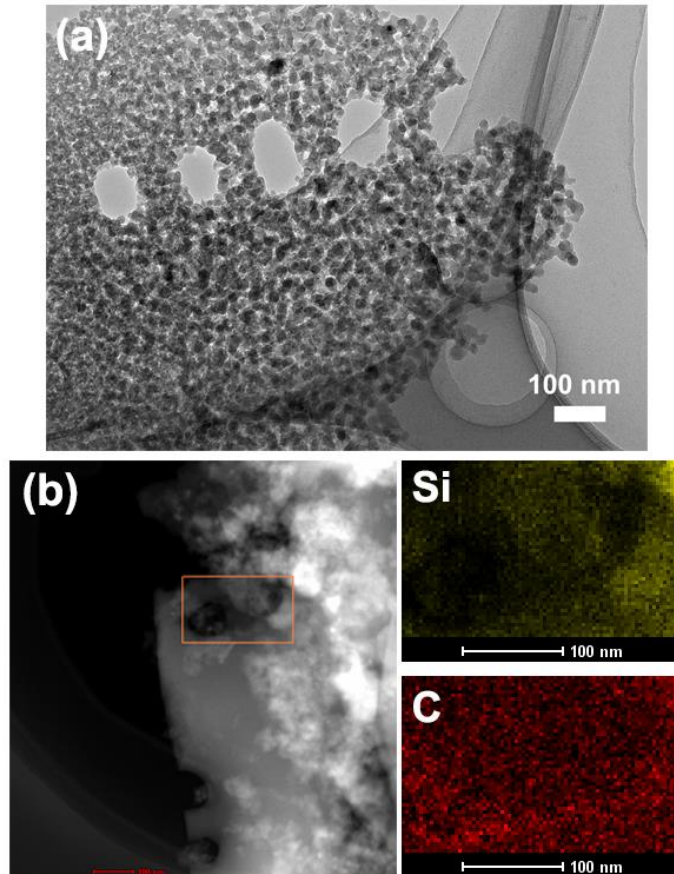


Fig.S6 (a) Si/SiO₂ after magnesiothermic reduction under 640 °C for 1 h. (b) HAADF characterizations of the Si/SiO₂@C (13%) composite material and on the right side is the element mappings for the distribution of Si and C, respectively.

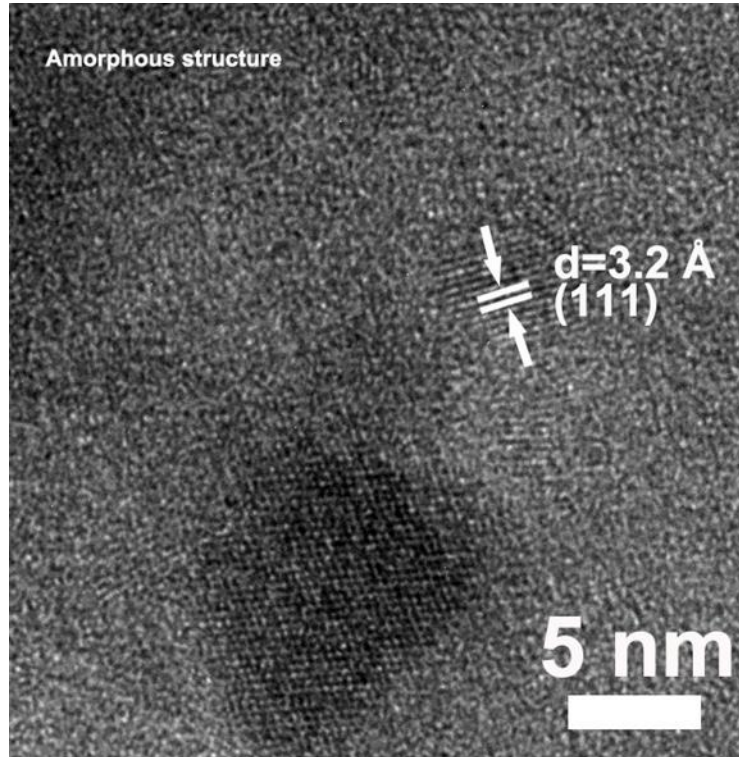


Fig.S7 HR-TEM characterization of the Si/SiO₂@C (13%) composite material.

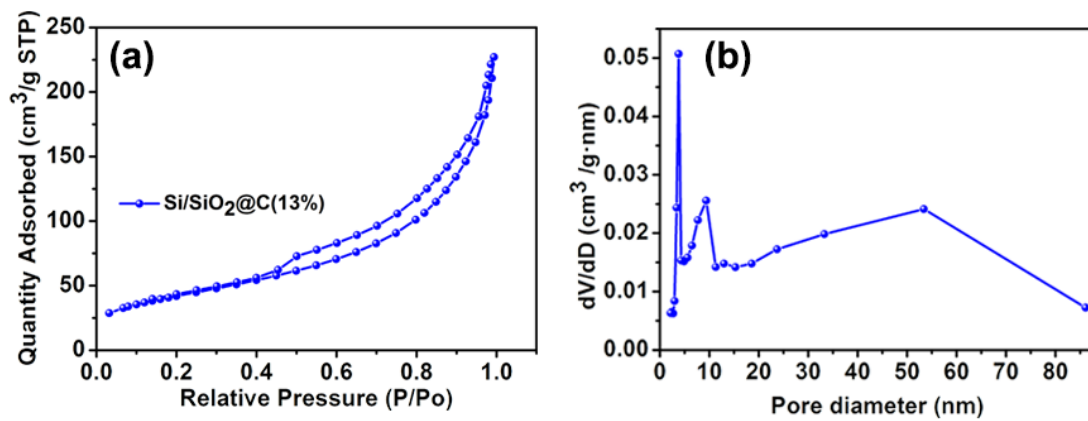


Fig.S8 (a) N₂ adsorption/desorption isotherm curves of the Si/SiO₂@C (13%) composite material. (b) The Barrett-Joyner-Halenda (BJH) pore size distributions from adsorption branches of the isotherm.

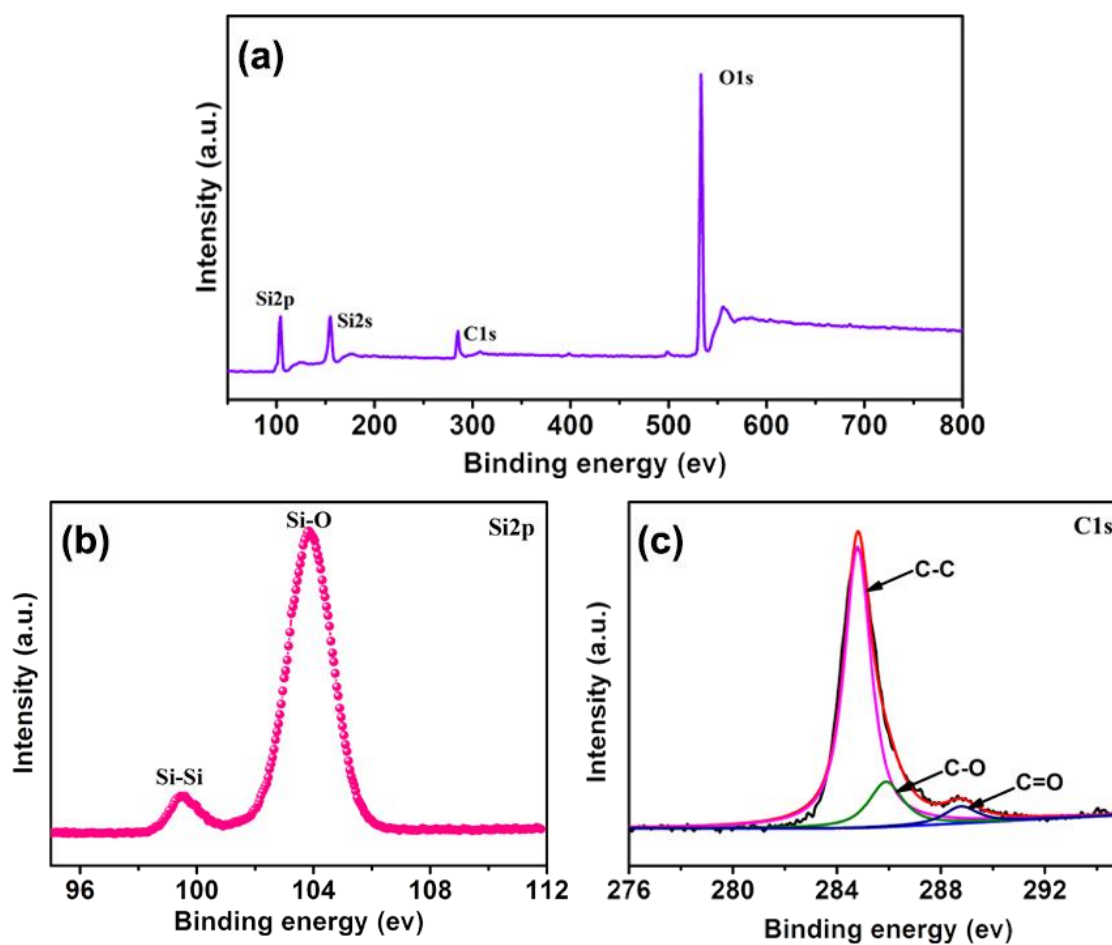


Fig.S9 (a) XPS survey scan spectrum of Si/SiO₂@C (13%) composite material, the corresponding high-resolution XPS spectra of (b) Si 2p, (c) C 1s.

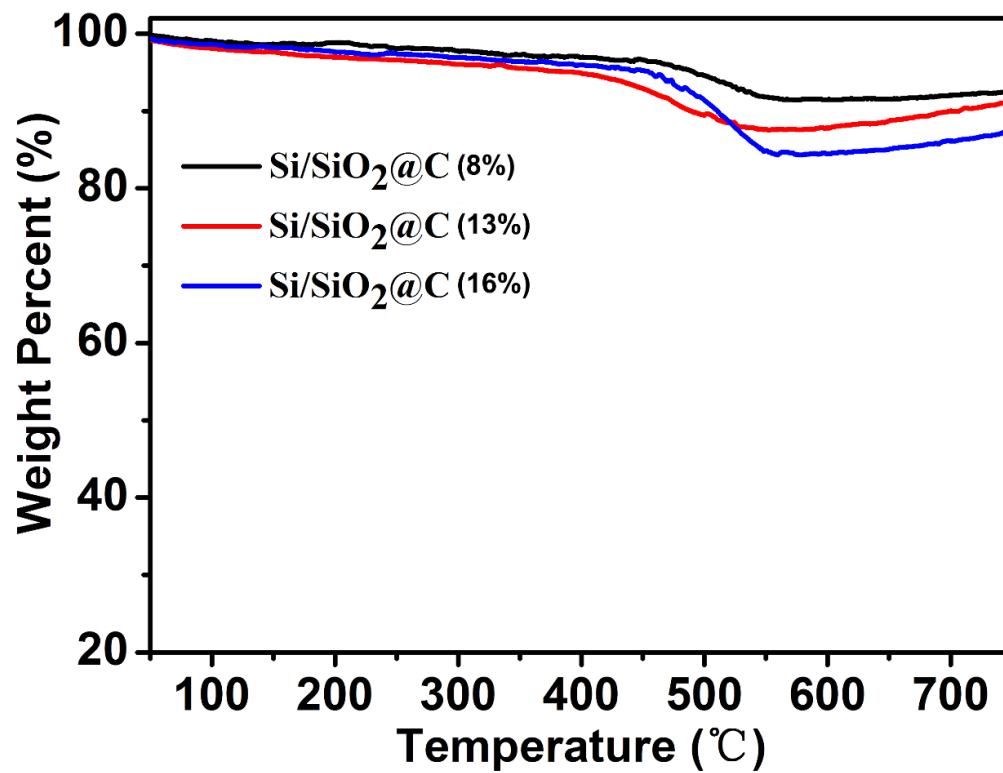


Fig.S10 Thermogravimetric analysis (TGA) curve of the Si/SiO₂@C composite materials with different content of carbon.

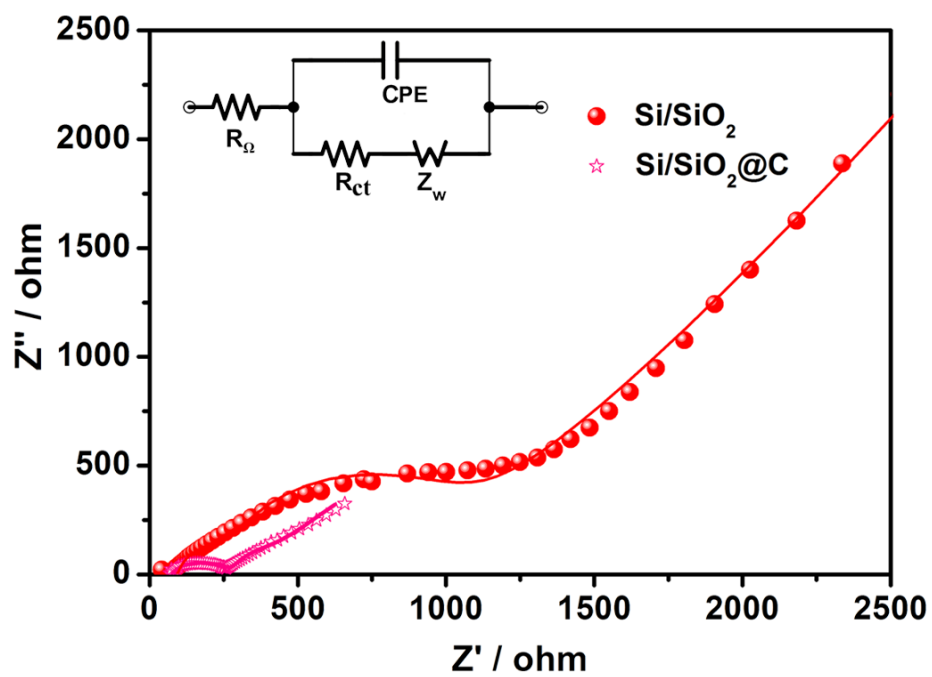


Fig.S11 Nyquist plots of the two electrodes after 200 cycles and the equivalent circuit (inset image) for fitting the impedance spectra. The solid lines are the fitted results.

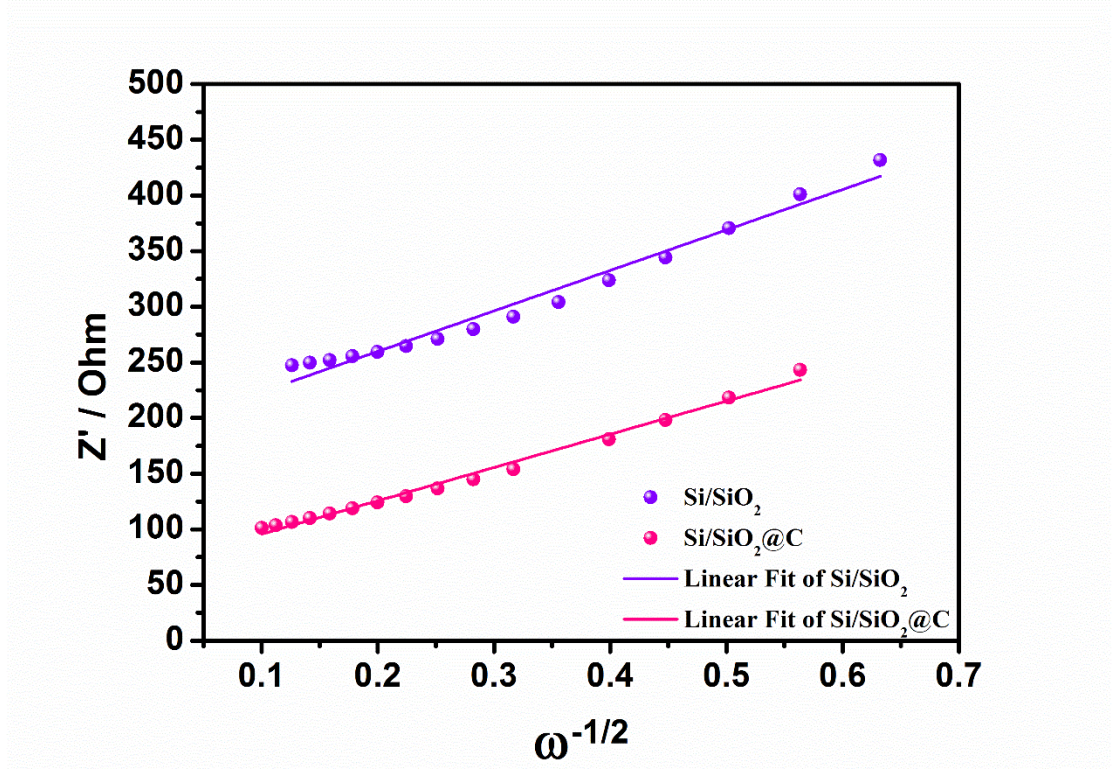


Fig.S12 The relationship between Z' and $\omega^{-1/2}$ at a very low frequency region.

The lithium ion diffusion coefficient can be calculated according to the Equations as following:

$$D = \frac{R^2 T^2}{2A^2 n^4 F^4 C^2 \sigma^2} \quad (1)$$

$$Z' = R_e + R_{ct} + \sigma \omega^{-1/2} \quad (2)$$

where A is the surface area of the electrode, n is the number of the electrons per molecule joining electrochemical reaction, F is the Faraday constant, C is the concentration of lithium ion in the electrode, R is the gas constant, T is the absolute temperature, ω is the angular frequency, and σ is the slope of the line Z' versus $\omega^{-1/2}$ after linear fitting (Fig.S12).^{1,2}

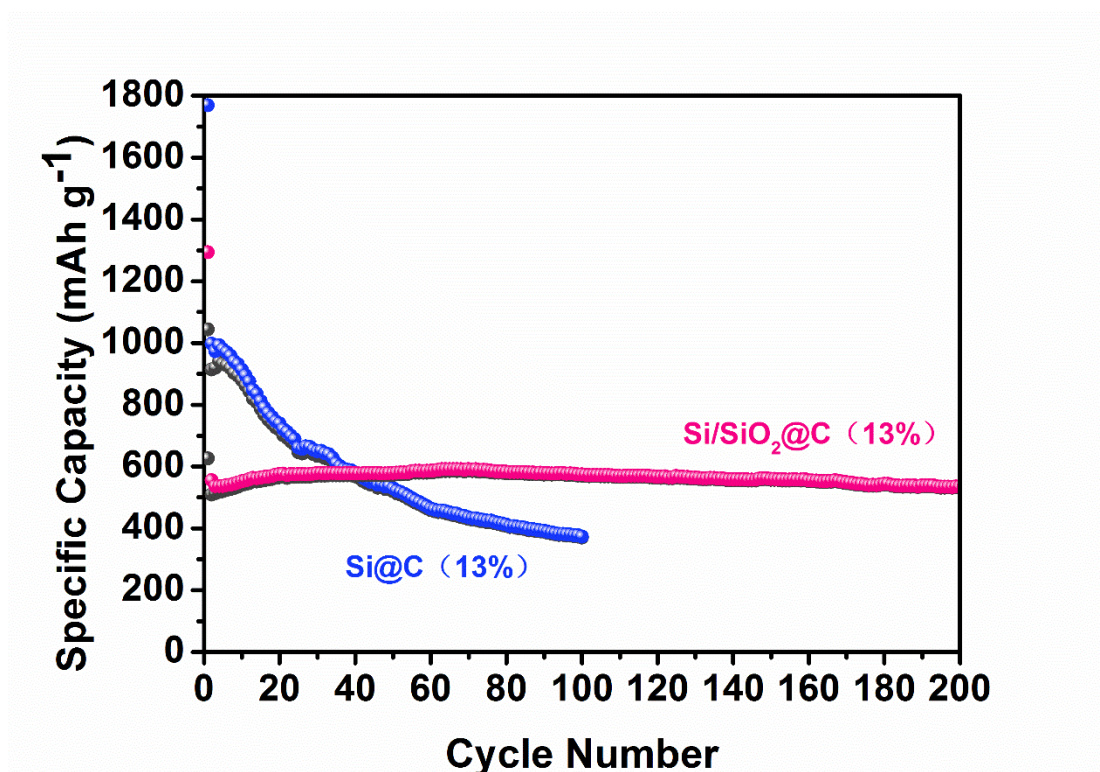


Fig.S13 Electrochemical cycling performances of the Si/SiO₂@C(13%) and Si@C(13%) composite materials at a current density of 500 mA/g after the first cycle activation at 50 mA/g between 0.01 and 1.5 V.

Table S1. Surface analysis data

Sample	Specific surface area [m ² g ⁻¹] ^{a)}	Average pore size [nm] ^{b)}	Pore volume [cm ³ g ⁻¹]
DE	49.86	6.20	0.08
620 °C	349.33	7.70	0.67
640 °C	398.97	5.96	0.59
660 °C	330.51	7.84	0.65
680 °C	260.74	8.06	0.53
Si/SiO ₂ @C (13%)	151.39	9.15	0.34

^{a)}Specific surface area was calculated from the linear part of BET plot; ^{b)} Average pore diameter was estimated from the Barrett–Joyner–Halenda formula.

References:

1. X. Wang, H. Hao, J. Liu, T. Huang and A. Yu, *Electrochim. Acta*, 2011, **56**, 4065.
2. S. Chen, Z. Chen, X. Xu, C. Cao, M. Xia and Y. Luo, *Small*, 2018, **14**, 1703361.